


Review Paper

A Review of the Sonication-Assisted Exfoliation Methods for MoX₂ (X: S, Se, Te) Using Water and EthanolSihan WANG⁽¹⁾, Yanshu YU⁽²⁾, Jianling MENG^{(1)*}*College of Mathematics and Physics, Beijing University of Chemical Technology
Beijing, China; e-mails: wsh20010@163.com; 674991037@qq.com**Corresponding Author e-mail: mengjianling@buct.edu.cn*(received October 10, 2024; accepted December 18, 2024; published online March 7, 2025)*

Two-dimensional transition metal dichalcogenides (MoX₂, where X = S, Se, Te), have been the research hotspot over the past decade. The sonication-assisted liquid-phase exfoliation method is suitable for the mass production of MoX₂ in practical applications. Water and ethanol, rather than organic solvents, are increasingly chosen for liquid-phase exfoliation method due to their non-toxic, environmentally friendly properties. However, a systematic review of the method for MoX₂ preparation using water and ethanol is lacking. In this paper, recently published work on the sonication-assisted exfoliation method for MoX₂ preparation using water and ethanol is summarized. Three key parameters are focused on: solvents selection, sonication power, and sonication time. Finally, the application of MoX₂ flakes and the future outlook of the sonication-assisted liquid-phase exfoliation method using water and ethanol are presented. The review aims to provide guidance on exfoliating MoX₂ using the sonication-assisted exfoliation method with water and ethanol.

Keywords: two-dimensional transition metal dichalcogenides; sonication-assisted liquid-phase exfoliation; water; ethanol.



Copyright © 2025 The Author(s).
This work is licensed under the Creative Commons Attribution 4.0 International CC BY 4.0
(<https://creativecommons.org/licenses/by/4.0/>).

1. Introduction

Since graphene was discovered by [NOVOSELOV *et al.* \(2004\)](#), two-dimensional (2D) materials have become a hotspot in materials research. So far, various 2D materials have been studied, including the insulator boron nitride (BN), semiconductor transitional metal dichalcogenides (TMDs), magnetic materials such as CrX₃ (I, Br), Fe₃GeTe₂, and the topological insulator Bi₂Se₃, among others. TMDs MX₂ (where M = Mo, W, and X = S, Se) shows potential in many applications due to its excellent physical properties. For example, MoS₂-based field-effect transistors (FETs) exhibit a $\sim 10^8$ on/off ratio with mobility $\sim 200 \text{ cm}^2\text{V}^{-1}\text{s}^{-1}$ ([RADISAVLJEVIC *et al.*, 2011](#)). Monolayer MoS₂ also demonstrates a strong photoluminescence effect due to the indirect-to-direct bandgap transition (from 1.9 eV to 2.2 eV) from bulk to monolayer ([MAK *et al.*, 2010](#)). Actually, monolayer MoS₂ exists in three distinct phases: the semiconductive 2H phase, the

metallic 1T phase, and the 1T' phase. The 2H-MoS₂ phase holds potential development for applications in valleytronics. On one hand, 2H-MoS₂ displays a novel valley degree of freedom due to broken inversion symmetry. On the other hand, its valley and spin degrees of freedom are coupled due to spin-orbit splitting ([XIAO *et al.*, 2012](#)). MoSe₂ is more conductive with respect to MoS₂ due to selenium (Se) atoms being more conductive than molybdenum (Mo) atoms. The bandgaps of monolayer MoSe₂ and MoTe₂ are 1.55 eV, 1.1 eV, respectively, extending the spectral range of TMDs from the visible to near-infrared region ([WU *et al.*, 2020](#)).

The mass production of TMDs is required for their practical applications. Currently, there are two categories of TMDs synthesis methods: bottom-up and top-down approaches. Chemical vapor deposition (CVD) and metal-organic chemical vapor deposition (MOCVD), both of which are bottom-up approaches, can synthesize wafer-scale monolayer MoX₂ films. Although continuous efforts to produce large-scale wafers

show promise for practical applications (YU *et al.*, 2017; HU *et al.*, 2023; XU *et al.*, 2021), the cost remains high for industrial application at this stage. The mechanical exfoliation approach, a top-down approach, can produce high-quality MoX_2 , which is suitable for advanced fundamental research. However, its efficiency is relatively low. Another top-down approach is the liquid-phase exfoliation (LPE). LPE methods include shear exfoliation, ultrasonication exfoliation, and microfluidization exfoliation (SETHULEKSHMI *et al.*, 2024). Sonication-assisted liquid exfoliation is the most common technique for MoX_2 synthesis. For example, COLEMAN *et al.* (2011) demonstrated the feasibility of ultrasonic-assisted liquid-phase exfoliation as early as 2011. Their findings were further supported and expanded upon in subsequent studies (KHAN *et al.*, 2011; 2012; O'NEILL *et al.*, 2011; BARWICH *et al.*, 2013; COLEMAN *et al.*, 2013; HANLON *et al.*, 2015; GHOLAMVAND *et al.*, 2016; BACKES *et al.*, 2017; HARVEY *et al.*, 2017; SYNNATSCHKE *et al.*, 2019; GRIFFIN *et al.*, 2020). Though the sonication-assisted liquid exfoliation process can cause problems such as high defect rate, low stability and impaired electronic properties of the nanosheets, its advantages are: (1) simplicity, universality, and low cost, making it suitable for mass production (AKEREDOLU *et al.*, 2024); (2) mild operating conditions (room temperature and pressure) (AGGARWAL *et al.*, 2024), and the properties of the nanosheets being controllable by adjusting process parameters (SETHULEKSHMI *et al.*, 2024).

The common solvents used in sonication-assisted liquid exfoliation for MoX_2 synthesis are organic polymer, typically N-methyl-2-pyrrolidone (NMP) (O'NEILL *et al.*, 2012). However, the polymer is toxic and hard to remove due to its generally high boiling point. Similarly, although alternative surfactant can exfoliate MoS_2 by expanding the layers, the surfactant molecules are usually difficult to recycle (MA *et al.*, 2018; POZZATI *et al.*, 2024). Recently, significant efforts have been devoted to utilizing green solvents that achieve comparable concentrations and sizes of TMDs dispersion as NMP and surfactant-based solvents. It has been demonstrated that phyto-extracted green solvents facilitate the production of few layer MoS_2

which enhances the photo-conversion efficiency of dye-sensitized solar cells and exhibits an excellent redox activity with high specific capacitance (KUMAR *et al.*, 2023). Polarclean, Iris and Cyrene have been reported as the most promising green solvents for the production of graphene, MoS_2 and WS_2 . In particular, Polarclean has been highlighted due to its low defect density (OCCHIUZZI *et al.*, 2023). RAFI *et al.* (2024) produced bilayered and trilayered MoS_2 nanosheets by employing isopropyl alcohol and deionized water in a 7:3 ratio as a cosolvent. Green solvents biomaterials are beyond the scope of this review, with relevant work summarized in other reviews (SETHULEKSHMI *et al.*, 2024). Among organic solvents, ethanol is considered more environmentally favorable based on environmental impact, health, and safety (EHS) statements (CAPELLO *et al.*, 2007; SHELDON *et al.*, 2019). Hence, our review focuses on water and ethanol solvents.

To our knowledge, no review has been reported on the sonication-assisted liquid exfoliation of MoX_2 employing water and/or alcohol, specifically in terms of factors of process, although reviews on water-mediated exfoliation of MoS_2 have been reported (AGGARWAL *et al.*, 2024).

Our review summarizes the sonication-assisted exfoliation formulation using water and/or ethanol from the following three aspects: solvents selection, sonication power, and sonication time, aiming to provide a guidance on exfoliating TMDs using water and/or ethanol via the sonication-assisted exfoliation method.

2. Sonication-assisted exfoliation recipe

A typical sonication-assisted exfoliation process is as follows (Fig. 1). Firstly, MoX_2 powder is mixed with appropriate solvents. Then, the mixture is ultrasonicated in ultrasonic instrument. Various techniques are used to prevent excessive temperature rise during sonication. For instance, intermittent ultrasound, for example, 40 seconds ultrasonic time followed by 20-second break time, are utilized. Additionally, an ice bath or water-cooling temperature control system is used to maintain a constant temperature. The resulting dispersion subsequently is centrifuged, and the

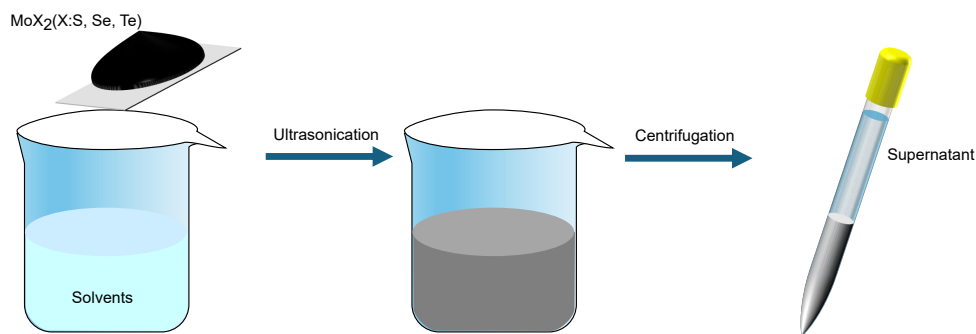


Fig. 1. Schematic diagram of the sonication-assisted exfoliation process.

supernatant is extracted. The speed and number of centrifugation steps help to roughly separate the MoX₂ flakes by size.

The mechanism underlying the sonication-assisted exfoliation process has been reported (GUPTA *et al.*, 2016; COLEMAN *et al.*, 2011; SMITH *et al.*, 2011; NICOLSI *et al.*, 2013; LI *et al.*, 2020). The materials discussed in detail are graphite, and the LPE solvents used are various organic solvents, such as IPA/H₂O mixture, sodium dodecylbenzenesulfonate (SDBS)/H₂O mixture and NMP (LI *et al.*, 2020). Actually, LPE involves two simultaneous structural modifications: exfoliation (reduction in thickness), and fragmentation (reduction in lateral dimension). The research explains exfoliation and fragmentation processes in detail. It was found that fragmentation and exfoliation take place during LPE in three distinct stages, with the kink-band-induced peeling process being one key stages (shown in Fig. 2). In the first stage, graphite flake rupture along existing defects, and kink bands are formed due to surface acoustic waves. The second stage involves the kink bands leading to increase in chemical activity, which promotes fragmentation and exfoliation, leading to the peeling off thin graphite stripes. Then, the last stage involves the peeled graphite strips being exfoliated into thin flakes, with a minimum of ~30 layers. Although the research did not discuss exfoliation of MoX₂ by LPE using water and/or ethanol, the mechanism is also applicable to the exfoliation of MoX₂ by LPE using organic solvents, as both materials possess analogous 2D layered structures.

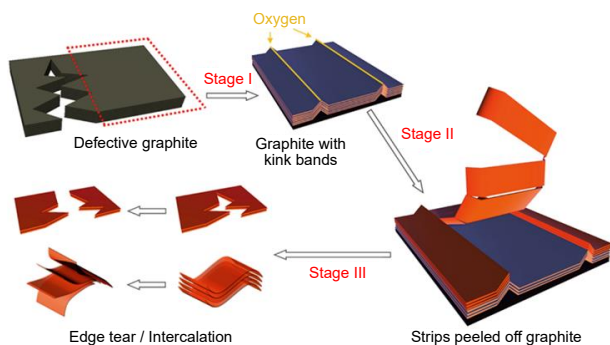


Fig. 2. Schematic diagram of the sonication-assisted LPE mechanism of graphite (reprinted with permission from (LI *et al.*, 2020)).

In general, the abovementioned procedures all have influence on the concentration and size of the exfoliated MoX₂ flakes. Here, we focus on three main influencing factors, including solvents selection, sonication power and sonication time, while other aspects are beyond the scope of this review.

2.1. Solvents selection

There are several theories for screening solvents, such as Hansen solubility parameters (HSP), Young's equation, and Shen's method for probing and matching surface tension components (MA *et al.*, 2020). The HSP theory is commonly used, with the HSP distance R_a employed to evaluate the level of dissolution process between solvents and solutes, as described by the following equation:

$$R_a = [4(\delta_{D,\text{solv}} - \delta_{D,\text{solu}})^2 + (\delta_{P,\text{solv}} - \delta_{P,\text{solu}})^2 + (\delta_{H,\text{solv}} - \delta_{H,\text{solu}})^2], \quad (1)$$

where δ_D , δ_P , δ_H represent dispersive, polar, and hydrogen-bonding solubility parameters of a solvent and solutes, respectively (ZHOU *et al.*, 2011). The reference HSP parameters of MoX₂, H₂O, and ethanol are shown in Table 1.

In general, pure water is a poor solvent for MoS₂ exfoliation. However, MA *et al.* (2018; 2020) demonstrated the feasibility of exfoliating MoS₂ using water. The authors concluded that the stability of MoS₂ in an aqueous solution is due to the fragmentation of the MoS₂ flakes induced by sonication. Compared to graphite, MoS₂ is easier to fragment. The obtained MoS₂ nanosheets have sizes ranging from 100 nm to 400 nm with a few layers (5–6 layers) or multilayers (15–20 layers) in thickness. Mesoporous sheets were also observed (shown in Fig. 3a). LI *et al.* (2015) reported that MoS₂ can be exfoliated in pure water due to defects and enlarged interlayer spacing induced by the fabrication process. ZHAO *et al.* (2016) exfoliated commercial MoS₂ in water using a specially designed sonication instrument with a stirring function. The slipping exfoliation was achieved by the tilted rotation of MoS₂ sheets during stirring. FORSBERG *et al.* (2016) exfoliated MoS₂ in water using a two-step method. First, an orbital sander was used for mechanical ex-

Table 1. HSP value for MoX₂, H₂O, and ethanol.

	δ_D (0.5 MPa)	δ_P (0.5 MPa)	δ_H (0.5 MPa)
MoS ₂ (ZHOU <i>et al.</i> , 2011)	17–19	6–12	4.5–8.5
MoSe ₂ (MAO <i>et al.</i> , 2018)	15.3–18.4	9–18	3.3–11.3
MoTe ₂ (CUNNINGHAM <i>et al.</i> , 2012)	17.8	8	6.5
H ₂ O (ZHOU <i>et al.</i> , 2011)	15.8	8.8	19.4
Ethanol (ZHOU <i>et al.</i> , 2011)	18.1	17.1	16.9

*The HSP parameters are obtained from (ZHOU *et al.*, 2011). Republished with permission from Angewandte Chemie International Edition, permission conveyed through Copyright Clearance Center, Inc.

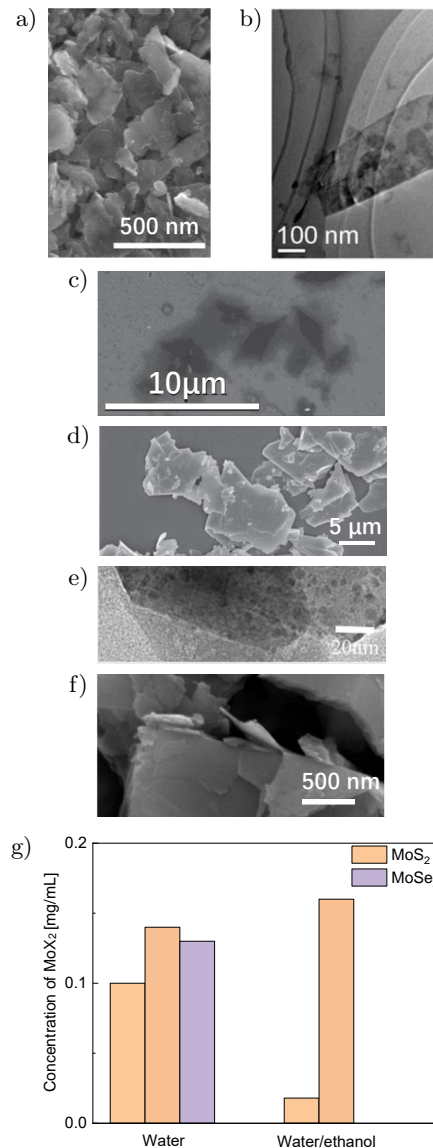


Fig. 3. Scanning electron microscope (SEM) images of exfoliated MoS₂ flake (a–f) except for (e), which is the transmission electron microscope (TEM) image of exfoliated MoS₂ with various vol% ethanol/water solvents. The concentration of MoX₂ using water and water/ethanol solvents is shown in (g).

(a) Reprinted from (MA *et al.*, 2018) with permission from Elsevier; (b) republished with permission from *Angewandte Chemie International Edition* from ZHOU *et al.* (2011), permission conveyed through Copyright Clearance Center, Inc; (c) republished with permission from *IEEE Transactions on Nanotechnology* from YUAN *et al.* (2021), permission conveyed through Copyright Clearance Center, Inc; (d) reprinted from WANG *et al.* (2013) with permission from Elsevier; (e) republished with permission from *Journal of Materials Science: Materials in Electronics* from YANG *et al.* (2017), permission conveyed through Copyright Clearance Center, Inc; (f) adapted with permission from TAGHAVI and AFZALZADEH (2021), Creative Commons License CC BY-SA 4.0.

foliation of MoS₂. Then, the obtained MoS₂ powder was exfoliated in water by sonication. MoS₂ was also exfoliated in water via sonication under an Ar/H₂ at-

mosphere (GUTIÉRREZ, HENGLEIN, 1989). LIU *et al.* (2018a) found that bulk MoSe₂ can be directly exfoliated in hot water at 50 °C, achieving intense exfoliation kinetics while maintaining high quality. Based on simulation at atomic and molecular scales, it was proposed that the stable dispersion of MoSe₂ nanosheets in water is achieved owing to the presence of platelet surface charges originating from edge functionalization and intrinsic polarity. A large number of atomically thin MoSe₂ layers are produced by 100 W sonication for 24 h and 8000 rpm centrifugation for 40 min. The lateral dimensions of the obtained MoSe₂ nanosheet range from 50 nm to 500 nm. A large proportion (>70 %) of these layers are less than 2.0 nm thick, and >40 % of them are thinner than 1.0 nm, corresponding to monolayers. Other studies have reported that atomically thin MoSe₂ platelets can be exfoliated from bulk MoSe₂ by 20 W sonication for 60 h and dispersed in pure water by centrifugation for 30 min under temperature control (KIM *et al.*, 2015). The exfoliated flakes have dimensions of 200 nm to 300 nm with 2–3 layers. The concentration is shown in Fig. 3g, and lateral size and number of layers of exfoliated MoX₂ using water as the solvent are shown in Fig. 4, with data coming from the above-mentioned studies.

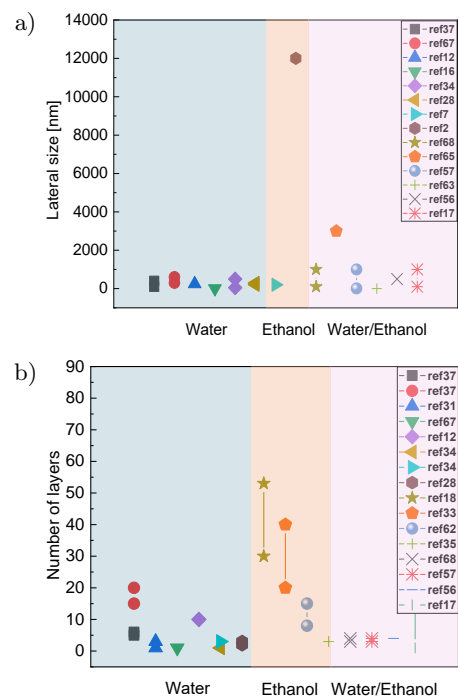


Fig. 4. MoX₂ using water, ethanol and water/ethanol solvents: a) lateral size; b) number of layers.

Anhydrous ethanol is used as the initial solvent for exfoliating MoSe₂ and MoTe₂. MoSe₂ nanosheets were obtained in anhydrous ethanol through the ultrasonic-assisted LPE method and were subsequently used as a gas sensor as the ethanol solvent evaporates (CHEN *et al.*, 2019). Absolute alcohol has also been reported

to be used in the preparation of MoTe₂ nanoflakes (HAN *et al.*, 2023; LIANG *et al.*, 2020). Exfoliation was obtained by sonication for 20 h followed by centrifugation. At the end of the process, the layer thickness of the stripped nanosheet ranged from 30 to 53 atomic layers (HAN *et al.*, 2023). Similarly, YAN *et al.* (2018) mixed bulk MoTe₂ powders with anhydrous alcohol and sonicated powders for 12 h. After centrifugation and additional processing, the number of layers of the resulting MoTe₂ ranged from 8 to 15. AHMAD *et al.* (2021) reported MoTe₂ nanosheets with a lateral size of about 12 μm by sonicating the mixture of MoTe₂ powder and absolute ethanol for 16 h. MoTe₂ nanosheets were also prepared with an ethanol-assisted ultrasound-assisted liquid-phase exfoliation (UALPE) method at 20 °C (LIU *et al.*, 2018b). The concentration is shown in Fig. 3g, and lateral size and number of layers of exfoliated MoX₂ using ethanol solvent are shown in Fig. 4.

Besides single-component solvents, the HSP theory can also be used for solvent mixtures. The HSP parameters of a mixture are a linear combination of the corresponding parameters of each component, as follows:

$$\delta_{\text{blend}} = \sum \phi_{n,\text{comp}} \delta_{n,\text{comp}}, \quad (2)$$

where δ_{blend} , $\phi_{n,\text{comp}}$, $\delta_{n,\text{comp}}$ represent the HSP parameters of the blend, the volume fraction of each component, and the HSP parameters of each component, respectively (ZHOU *et al.*, 2011). By choosing water and/or alcohol with the appropriate composition, a high dispersion concentration of MoS₂ can be achieved. Experimental results and theoretical predictions are consistent in showing that a 45 vol% ethanol/water provides the highest dispersion concentration, with a value of 0.018 ± 0.003 mg/mL, which is approximately 13 times higher than that in pure ethanol and 68 times higher than that in pure water (ZHOU *et al.*, 2011). The size of the sheets varies from 100 nm to several micrometers and their thickness is 3–4 layers (shown in Fig. 3b). Other works also report using a 45 vol% alcohol/water mixture as the solvent for MoS₂ flake preparation. YUAN *et al.* (2021) prepared MoS₂ nanosheets by liquid phase exfoliation (LPE) for a formic acid gas sensor using a 45 vol% alcohol/water mixture as the solvent. The size of the nanosheets obtained is about 3 μm (shown in Fig. 3c). WANG *et al.* (2013) also prepared MoS₂ nanosheets by dispersing MoS₂ powder in a 45 vol% ethanol/water mixture, with a thickness of 3–4 layers and the size of nanosheets ranging from tens of nanometers to several micrometers (shown in Fig. 3d). HUANG *et al.* (2024) prepared few-layer MoS₂ flakes with an average thickness of 7 nm by sonication in 45 vol% ethanol/water mixture at 240 W for 90 min. In addition to the 45 vol% ethanol/water mixture, other proportions of ethanol/water have also been reported for liquid-phase exfoliation of MoS₂ flakes.

For example, MoS₂ quantum dots were obtained by dispersing defected MoS₂ nanosheets into a 25 vol% ethanol/water solution. Due to the inherent defects in MoS₂, the average lateral size of acquired MoS₂ quantum dots is 3.6 nm – shown in Fig. 3e (YANG *et al.*, 2017). A 23 vol% ethanol/deionized water solution was also reported to be utilized to exfoliate MoS₂, yielding flakes with an average of 4 layers and a lateral size of 500 nm – shown in Fig. 3f (TAGHAVI *et al.*, 2021). Furthermore, a 50 vol% ethanol/water solvent mixture has been reported to exfoliate MoS₂, resulting in nanosheets with lateral sizes of several micrometers and damaged surface edges (PRABUKUMAR *et al.*, 2018; JIN *et al.*, 2020). Compared to the same proportion of NMP/water, this exfoliation efficiency is poor (PRABUKUMAR *et al.*, 2018). HALIM *et al.* (2013) used Young's equation to determine the liquid-solid interfacial energy and predicted that the optimal cosolvent of alcohol-water mixtures should have a surface tension between 30 mJ/m² and 35 mJ/m². The concentration lateral size and number of layers of exfoliated MoX₂ using water/ethanol solvent are shown in Figs. 3g and 4, respectively.

2.2. Sonication power

In addition to the solvent type, which affects the quality of the final MoX₂ production in ultrasound-assisted liquid exfoliation, the ultrasonic power also plays a crucial role. Sonication power is an important parameter influencing the exfoliation process. The size of exfoliated MoS₂ flakes increases as the sonication power increases from 38.5 W, 47 W, to 65.5 W with bath sonication. At 84 W, the MoS₂ flakes begin to agglomerate (TAGHAVI, AFZALZADEH, 2021). This phenomenon can be explained by the collapse of the high-energy bubbles, which increases the size and number of bubbles. As a result, the shock waves produced by sonication are reduced while the bubble implosions increase. Unlike bath sonication, probe sonication uses an ultrasound probe to transmit vibrations. HAU *et al.* (2021) synthesized MoS₂ for 8 h via probe sonication at 420 W using a water/ethanol with a volume ratio of 2:1.

Some divergence exists between sonication-assisted LPE using water and/or ethanol and organic solvents. For instance, using a mixture of chloroform and acetonitrile in a 65:35 ratio as solvents for LPE, the average size of MoS₂ nanosheets decreases as the ultrasonic power increases from 350 W, 450 W to 550 W. Meanwhile, the concentration of produced MoS₂ increases correspondingly. This phenomenon is explained by the cavitation effect and micro-jet effect induced by ultrasound. The cavitation effect is the primary force for exfoliating layered MoS₂, involving the process of the formation, growth, and implosive collapse of bubbles. Simultaneously, the micro-jet effect induced by the collapse of bubbles is the force that fragments the

MoS₂ sheets (ZHANG *et al.*, 2014). The effect of ultrasonic power on exfoliation has also been studied using NMP as a solvent (QIAO *et al.*, 2014). The ultrasonic power was controlled from 100 W, 200 W, 250 W, 285 W, 320 W, 350 W to 400 W. The concentration of nanosheets increased as the sonication power increased, and then decreased after 320 W. Meanwhile, the size of the nanosheets initially decreased and then increased after 320 W. This behavior is associated with the ultrasonic cavitation effect. At low input power, the covalently bonded S-Mo-S sheet are broken into small flakes due to inertial cavitation. However, at high input power, the breaking intensity decreases due to fewer large bubbles being generated, a phenomenon known as ultrasonic cavitation shielding effect.

2.3. Sonication time

Sonication time is another important parameter. TAGHAVI and AFZALZADEH (2021) systematically studied the effect of sonication time on the exfoliation of MoS₂ using a mixture of 77 % deionized (DI) water and 23 vol% ethanol by volume. They found that the size of MoS₂ flakes increases as the effective sonication time increases from 15 min to 60 min, but then decreases with prolonged sonication time. This is due to the agglomeration process. A similar effect has been observed in the LPE of MoS₂ using NMP (O'NEILL *et al.*, 2012). The dimensions of MoS₂ flakes increase after 23 h of sonication, reaching a maximum after 60 h, and then decrease after 60 h of sonication. MITTAL *et al.* (2023) reported that the number of exfoliated MoSe₂ layers in DI water and ethanol decreases as the sonication time increases from 10 min to 60 min. LIU *et al.* (2018a) studied the effect of sonication time on exfoliation of MoSe₂ using water at 50 °C. For comparison, the authors sonicated bulk MoSe₂ for 8 h and 24 h, and found that the layers after 8 h of sonication could withstand higher centrifugal speed. However, bulk MoSe₂ could be broken into high-quality layers at a longer ultrasound time (24 h) due to more sufficient exfoliation.

XU *et al.* (2024) first compared the effects of different ethanol contents on the dispersibility of MoTe₂, and then analyzed the relationship between sonication time and the thickness of nanosheets at intervals of 0.5 h, 1.5 h, 2.5 h, 3.5 h, 4.5 h, and 5.5 h. The results showed that the average thickness of the nanosheets decreased as the sonication time increased.

3. Application, perspective and conclusions

Exfoliated TMDs using water and/or ethanol solvents enable a wide range of applications, such as electrochemical application as supercapacitor electrodes, photoelectrochemical applications for photocurrent response material (KAJBAFVALA *et al.*, 2018), mechani-

cal reinforcement in polymers (O'NEILL *et al.*, 2012), electrocatalysts for hydrogen evolution reactions, hazardous gas sensor, batteries, surface coatings, and more. Due to its high carrier mobility, strong spin-orbit coupling, and extensive light absorption, MoSe₂ is considered as one of the most promising materials for optoelectronics in TMDs, making it suitable for flexible, lightweight optoelectronic devices (PATEL *et al.*, 2019). MoSe₂ exfoliated by alcohol solvents can also be applied to gas sensors by taking advantage of the volatilization of alcohol (ZHOU *et al.*, 2011). MoTe₂ can be transformed into many types of lasers following specific processing. Additionally, sonication-assisted LPE using water and/or ethanol solvents is an environment-friendly, low-cost, and easy-to-operate method for scaling up mass production of TMD flakes, making it suitable for industrial practical applications (CIESIELSKI, SAMORÌ, 2014). Non-toxic, environmentally friendly solvents and dispersants can extend the range of 2D TMD inks (LEE *et al.*, 2020). From a technological perspective, sonication-assisted LPE using water and ethanol not only facilitates upscaled production of TMDs flakes comparable to organic solvents, but it is also an economical and practical solution, as water and ethanol do not require additional post-processing for environmental compliance.

In this review, the preparation of MoX₂ flakes using the sonication-assisted LPE method with water and/or ethanol was summarized. Although many parameters influence this method, the review focused on three main parameters: solvent selection, sonication power, and sonication time. Solvent selection refers to the ratio of water and/or alcohol used. Related studies were summarized, revealing that a 45 vol% alcohol/water mixture is the optimal solvent for MoS₂, as explained by HSP theory. The effects of sonication power exhibit some inconsistencies, and even some divergences exist between LPE using water and/or ethanol solvents versus organic solvents. This variation may be attributed to differences in sonication equipment used by various research groups. Regarding sonication time, the size of MoS₂ flakes initially increases, and then decreases as sonication time increases. This phenomenon is analogous to that observed when using organic solvents. To further analyze the mechanism behind the LPE method using water and/or ethanol solvents, the advanced LPE mechanism, which includes three stages, is summarized from the literature. Finally, the wide applications of exfoliated MoX₂ flakes and the future outlook for the LPE method using water and ethanol solvents were discussed.

Acknowledgments

This work was supported by the National Natural Science Foundation of China under grant no. 12104281. All data generated or analyzed during this study are

included in this published article. The authors declare that they have no relevant financial or non-financial interests to disclose.

References

1. AGGARWAL R., SAINI D., MITRA R., SONKAR S.K., SONKER A.K., WESTMAN G. (2024), From bulk molybdenum disulfide (MoS_2) to suspensions of exfoliated MoS_2 in an aqueous medium and their applications, *Langmuir*, **40**(19): 9855–9872, <https://doi.org/10.1021/acs.langmuir.3c03116>.
2. AHMAD H. *et al.* (2021), Generation of four-wave mixing in molybdenum ditelluride (MoTe_2)-deposited side-polished fibre, *Journal of Modern Optics*, **68**: 425–432, <https://doi.org/10.1080/09500340.2021.1908636>.
3. AKEREDOLU B.J. *et al.* (2024), Improved liquid phase exfoliation technique for the fabrication of MoS_2 /graphene heterostructure-based photodetector, *Heliyon*, **10**(3): e24964, <https://doi.org/10.1016/j.heliyon.2024.e24964>.
4. BACKES C. *et al.* (2017), Guidelines for exfoliation, characterization and processing of layered materials produced by liquid exfoliation, *Chemistry of Materials*, **29**: 243–255, <https://doi.org/10.1021/acs.chemmater.6b03335>.
5. BARWICH S., KHAN U., COLEMAN J.N. (2013), A technique to pretreat graphite which allows the rapid dispersion of defect-free graphene in solvents at high concentration, *The Journal of Physical Chemistry C*, **117**(37): 19212–19218, <https://doi.org/10.1021/jp4047006>.
6. CAPELLO C., FISCHER U., HUNGERBÜHLER K. (2007), What is a green solvent? A comprehensive framework for the environmental assessment of solvents, *Green Chemistry*, **9**: 927–934, <https://doi.org/10.1039/B617536H>.
7. CHEN X. *et al.* (2019), Two-dimensional MoSe_2 nanosheets via liquid-phase exfoliation for high-performance room temperature NO_2 gas sensors, *Nanotechnology*, **30**: 445503, <https://doi.org/10.1088/1361-6528/ab35ec>.
8. CIESIELSKI A., SAMORÌ P. (2014), Graphene via sonication assisted liquid-phase exfoliation, *Chemical Society Reviews*, **43**(1): 381–398, <https://doi.org/10.1039/C3CS60217F>.
9. COLEMAN J.N. (2013), Liquid exfoliation of defect-free graphene, *Accounts of Chemical Research*, **46**(1): 14–22, <https://doi.org/10.1021/ar300009f>.
10. COLEMAN J.N. *et al.* (2011), Two-dimensional nanosheets produced by liquid exfoliation of layered materials, *Science*, **331**(6017): 568–571, <https://doi.org/10.1126/science.1194975>.
11. CUNNINGHAM G. *et al.* (2012), Solvent Exfoliation of transition metal dichalcogenides: Dispersibility of exfoliated nanosheets varies only weakly between compounds, *ACS Nano*, **6**(4): 3468–3480, <https://doi.org/10.1021/nm300503e>.
12. FORSBERG V. *et al.* (2016), Exfoliated MoS_2 in water without additives, *PLOS ONE*, **11**(4): e0154522, <https://doi.org/10.1371/journal.pone.0154522>.
13. GHOLAMVAND Z. *et al.* (2016), Comparison of liquid exfoliated transition metal dichalcogenides reveals MoSe_2 to be the most effective hydrogen evolution catalyst, *Nanoscale*, **8**: 5737–5749, <https://doi.org/10.1039/C5NR08553E>.
14. GRIFFIN A. *et al.* (2020), Effect of surfactant choice and concentration on the dimensions and yield of liquid-phase-exfoliated nanosheets, *Chemistry of Materials*, **32**(7): 2852–2862, <https://doi.org/10.1021/acs.chemmater.9b04684>.
15. GUPTA A., ARUNACHALAM V., VASUDEVAN S. (2016), Liquid-phase exfoliation of MoS_2 nanosheets: The critical role of trace water, *The Journal of Physical Chemistry Letters*, **7**(23): 4884–4890, <https://doi.org/10.1021/acs.jpcllett.6b02405>.
16. GUTIÉRREZ M., HENGLEIN A. (1989), Preparation of colloidal semiconductor solutions of MoS_2 and WSe_2 via sonication, *Ultrasonics*, **27**(5): 259–261, [https://doi.org/10.1016/0041-624X\(89\)90066-8](https://doi.org/10.1016/0041-624X(89)90066-8).
17. HALIM U. *et al.* (2013), A rational design of cosolvent exfoliation of layered materials by directly probing liquid-solid interaction, *Nature Communications*, **4**: 2213, <https://doi.org/10.1038/ncomms3213>.
18. HAN C. *et al.* (2023), Theoretical and experimental investigations on sub-nanosecond KTP-OPO pumped by a hybrid Q-switched laser with AOM and MoTe_2 saturable absorber, *Optics & Laser Technology*, **167**: 109760, <https://doi.org/10.1016/j.optlastec.2023.109760>.
19. HANLON D. *et al.* (2015), Liquid exfoliation of solvent-stabilized few-layer black phosphorus for applications beyond electronics, *Nature Communications*, **6**: 8563, <https://doi.org/10.1038/ncomms9563>.
20. HARVEY A. *et al.* (2017), Exploring the versatility of liquid phase exfoliation: producing 2D nanosheets from talcum powder, cat litter and beach sand, *2D Materials*, **4**: 025054, <https://doi.org/10.1088/2053-1583/aa641a>.
21. HAU H.H. *et al.* (2021), Enhanced NO_2 gas-sensing performance at room temperature using exfoliated MoS_2 nanosheets, *Sensors and Actuators A: Physical*, **332**(Part 1): 113137, <https://doi.org/10.1016/j.sna.2021.113137>.
22. HU J., ZHOU F., WANG J., CUI F., QUAN W., ZHANG Y. (2023), Chemical vapor deposition syntheses of wafer-scale 2D transition metal dichalcogenide films toward next-generation integrated circuits related applications, *Advanced Functional Materials*, **33**(40): 2303520, <https://doi.org/10.1002/adfm.202303520>.
23. HUANG C., ZHOU W., GUAN W., YE N. (2024), Molybdenum disulfide nanosheet induced reactive oxygen species for high-efficiency luminol chemiluminescence, *Analytica Chimica Acta*, **1295**: 342324, <https://doi.org/10.1016/j.aca.2024.342324>.

24. JIN X.-F. *et al.* (2020), Inkjet-printed MoS₂/PVP hybrid nanocomposite for enhanced humidity sensing, *Sensors and Actuators A: Physical*, **316**: 112388, <https://doi.org/10.1016/j.sna.2020.112388>.
25. KAJBAFVALA M., FARBOD M. (2018), Effective size selection of MoS₂ nanosheets by a novel liquid cascade centrifugation: Influences of the flakes dimensions on electrochemical and photoelectrochemical applications, *Journal of Colloid and Interface Science*, **527**: 159–171, <https://doi.org/10.1016/j.jcis.2018.05.026>.
26. KHAN U., O'NEILL A., PORWAL H., MAY P., NAWAZ K., COLEMAN J.N. (2012), Size selection of dispersed, exfoliated graphene flakes by controlled centrifugation, *Carbon*, **50**(2): 470–475, <https://doi.org/10.1016/j.carbon.2011.09.001>.
27. KHAN U., PORWAL H., O'NEILL A., NAWAZ K., MAY P., COLEMAN J.N. (2011), Solvent-exfoliated graphene at extremely high concentration, *Langmuir*, **27**(15): 9077–9082, <https://doi.org/10.1021/la201797h>.
28. KIM J. *et al.* (2015), Direct exfoliation and dispersion of two-dimensional materials in pure water via temperature control, *Nature Communications*, **6**: 8294, <https://doi.org/10.1038/ncomms9294>.
29. KUMAR B.A., ELANGOVAN, T., Raju, K., RAMALINGAM G., SAMBASIVAM S., ALAM M.M. (2023), Green solvent exfoliation of few layers 2D-MoS₂ nanosheets for efficient energy harvesting and storage application, *Journal of Energy Storage*, **65**: 107336, <https://doi.org/10.1016/j.est.2023.107336>.
30. LEE H. *et al.* (2020), Zwitterion-assisted transition metal dichalcogenide nanosheets for scalable and biocompatible inkjet printing, *Nano Research*, **13**: 2726–2734, <https://doi.org/10.1007/s12274-020-2916-4>.
31. LI X., WANG W., ZHANG L., JIANG D., ZHENG Y. (2015), Water-exfoliated MoS₂ catalyst with enhanced photoelectrochemical activities, *Catalysis Communications*, **70**: 53–57, <https://doi.org/10.1016/j.catcom.2015.07.024>.
32. LI Z. *et al.* (2020), Mechanisms of liquid-phase exfoliation for the production of graphene, *ACS Nano*, **14**: 10976–10985, <https://doi.org/10.1021/acsnano.0c03916>.
33. LIANG Y. *et al.* (2020), Nano-seconds pulsed Er:Lu₂O₃ laser using molybdenum ditelluride saturable absorber, *Optics & Laser Technology*, **121**: 105791, <https://doi.org/10.1016/j.optlastec.2019.105791>.
34. LIU Y.T., ZHU X.D., XIE X.M. (2018a), Direct exfoliation of high-quality, atomically thin MoSe₂ layers in water, *Advanced Sustainable Systems*, **2**(1): 1700107, <https://doi.org/10.1002/adsu.201700107>.
35. LIU X.J. *et al.* (2018b), Highly Active, durable ultrathin MoTe₂ layers for the electroreduction of CO₂ to CH₄, *Small*, **14**(16): 1704049, <https://doi.org/10.1002/smll.201704049>.
36. MA H. *et al.* (2020), Investigating the exfoliation behavior of MoS₂ and graphite in water: A comparative study, *Applied Surface Science*, **512**: 145588, <https://doi.org/10.1016/j.apsusc.2020.145588>.
37. MA H., SHEN Z., BEN S. (2018), Understanding the exfoliation and dispersion of MoS₂ nanosheets in pure water, *Journal of Colloid and Interface Science*, **517**: 204–212, <https://doi.org/10.1016/j.jcis.2017.11.013>.
38. MAK K.F., LEE C., HONE J., SHAN J., HEINZ T.F. (2010), Atomically thin MoS₂: A new direct-gap semiconductor, *Physical Review Letters*, **105**: 136805, <https://doi.org/10.1103/PhysRevLett.105.136805>.
39. MAO B., GUO D., QIN J., MENG T., WANG X., CAO M. (2018), Solubility-parameter-guided solvent selection to initiate Ostwald ripening for interior space-tunable structures with architecture-dependent electrochemical performance, *Angewandte Chemie International Edition*, **57**(2): 446–450, <https://doi.org/10.1002/anie.201710378>.
40. MITTAL H., RAZA M., KHANUJA M. (2023), Liquid phase exfoliation of MoSe₂: Effect of solvent on morphology, edge confinement, bandgap and number of layers study, *MethodsX*, **11**: 102409, <https://doi.org/10.1016/j.mex.2023.102409>.
41. NICOLOSI V., CHHOWALLA M., KANATZIDIS M.G., STRANO M.S., COLEMAN J.N. (2013), Liquid exfoliation of layered materials, *Science*, **340**(6139): 1226419, <https://doi.org/10.1126/science.1226419>.
42. NOVOSELOV K.S. *et al.* (2004), Electric field effect in atomically thin carbon films, *Science*, **306**(5696): 666–669, <https://doi.org/10.1126/science.1102896>.
43. OCCHIUZZI J., POLITANO G.G., D'OLIMPIO G., POLITANO A. (2023), The quest for green solvents for the sustainable production of nanosheets of two-dimensional (2D) materials, a key issue in the roadmap for the ecology transition in the flatland, *Molecules*, **28**(3): 1484, <https://doi.org/10.3390/molecules28031484>.
44. O'NEILL A., KHAN U., COLEMAN J.N. (2012), Preparation of high concentration dispersions of exfoliated MoS₂ with increased flake size, *Chemistry of Materials*, **24**(12): 2414–2421, <https://doi.org/10.1021/cm301515z>.
45. O'NEILL A., KHAN U., NIRMALRAJ P.N., BOLAND J., COLEMAN J.N. (2011), Graphene dispersion and exfoliation in low boiling point solvents, *The Journal of Physical Chemistry C*, **115**(13): 5422–5428, <https://doi.org/10.1021/jp110942e>.
46. PATEL A.B. *et al.* (2019), Electrophoretically deposited MoSe₂/WSe₂ heterojunction from ultrasonically exfoliated nanocrystals for enhanced electrochemical photoresponse, *ACS Applied Materials & Interfaces*, **11**(4): 4093–4102, <https://doi.org/10.1021/acsmi.8b18177>.
47. POZZATI M. *et al.* (2024), Systematic investigation on the surfactant-assisted liquid-phase exfoliation of MoS₂ and WS₂ in water for sustainable 2D material inks, *physica status solidi (RRL) – Rapid Research Letters*, **18**(9): 2400039, <https://doi.org/10.1002/pssr.202400039>.
48. PRABUKUMAR C., SADIQ M.M.J., BHAT D.K., BHAT K.U. (2018), Effect of solvent on the morphology of MoS₂ nanosheets prepared by ultrasonication-assisted exfoliation, *AIP Conference Proceedings*, **1943**: 020084, <https://doi.org/10.1063/1.5029660>.

49. QIAO W. *et al.* (2014), Effects of ultrasonic cavitation intensity on the efficient liquid-exfoliation of MoS₂ nanosheets, *RSC Advances*, **4**(92): 50981–50987, <https://doi.org/10.1039/C4RA09001B>.
50. RADISAVLJEVIC B., RADENOVIC A., BRIVIO J., GIACOMETTI V., KIS A. (2011), Single-layer MoS₂ transistors, *Nature Nanotechnology*, **6**: 147–150, <https://doi.org/10.1038/nnano.2010.279>.
51. RAFI R., RAHULAN K.M., FLOWER N.A.L., ABITH M., CHIDAMBARAM S.G.T., RAJENDRAN A.S. (2024), Optical limiting performance of MoS₂ nanosheets exfoliated via liquid-phase sonication: Implications for laser shielding, *ACS Applied Nano Materials*, **7**(10): 11097–11106, <https://doi.org/10.1021/acsnm.3c06096>.
52. SETHULEKSHMI A.S., JACOB F.P., JOSEPH K., APREM A.S., SISUPAL S.B., SARITHA A. (2024), Biomaterials assisted 2D materials exfoliation: Reinforcing agents for polymer matrices, *European Polymer Journal*, **210**: 112943, <https://doi.org/10.1016/j.eurpolymj.2024.112943>.
53. SHELDON R.A. (2019), The greening of solvents: Towards sustainable organic synthesis, *Current Opinion in Green and Sustainable Chemistry*, **18**: 13–19, <https://doi.org/10.1016/j.cogsc.2018.11.006>.
54. SMITH R.J. *et al.* (2011), Large-scale exfoliation of inorganic layered compounds in aqueous surfactant solutions, *Advanced Materials*, **23**(34): 3944–3948, <https://doi.org/10.1002/adma.201102584>.
55. SYNNAITSCHKE K. *et al.* (2019), Length- and thickness-dependent optical response of liquid-exfoliated transition metal dichalcogenides, *Chemistry of Materials*, **31**(24): 10049–10062, <https://doi.org/10.1021/acs.chemmater.9b02905>.
56. TAGHAVI N.S., AFZALZADEH R. (2021), The effect of sonication parameters on the thickness of the produced MoS₂ nano-flakes, *Archives of Acoustics*, **46**: 31–40, <https://doi.org/10.24425/aoa.2021.136558>.
57. WANG G.-X., BAO W.-J., WANG J., LU Q.-Q., XIA X.-H. (2013), Immobilization and catalytic activity of horseradish peroxidase on molybdenum disulfide nanosheets modified electrode, *Electrochemistry Communications*, **35**: 146–148, <https://doi.org/10.1016/j.elecom.2013.08.021>.
58. WU X., WANG Y.-h., LI P.-l., XIONG Z.-z. (2020), Research status of MoSe₂ and its composites: A review, *Superlattices and Microstructures*, **139**: 106388, <https://doi.org/10.1016/j.spmi.2020.106388>.
59. XIAO D., LIU G.-B., FENG W., XU X., YAO W. (2012), Coupled spin and valley physics in monolayers of MoS₂ and other group-VI dichalcogenides, *Physical Review Letters*, **108**: 196802, <https://doi.org/10.1103/PhysRevLett.108.196802>.
60. XU X. *et al.* (2021), Seeded 2D epitaxy of large-area single-crystal films of the van der Waals semiconductor 2H MoTe₂, *Science*, **372**(6538): 195–200, <https://doi.org/10.1126/science.abf5825>.
61. XU X. *et al.* (2024), High-Performance flexible broadband photoelectrochemical photodetector based on molybdenum telluride, *Small*, **20**(27): 2308590, <https://doi.org/10.1002/smll.202308590>.
62. YAN Z.Y. *et al.* (2018), MoTe₂ saturable absorber for passively Q-switched Ho₁Pr:LiLuF₄ laser at 3 μm, *Optics & Laser Technology*, **100**: 261–264, <https://doi.org/10.1016/j.optlastec.2017.10.012>.
63. YANG Q., HE Y., FAN Y., LI F., CHEN X. (2017), Exfoliation of the defect-rich MoS₂ nanosheets to obtain nanodots modified MoS₂ thin nanosheets for electrocatalytic hydrogen evolution, *Journal of Materials Science: Materials in Electronics*, **28**: 7413–7418, <https://doi.org/10.1007/s10854-017-6430-8>.
64. YU H. *et al.* (2017), Wafer-scale growth and transfer of highly-oriented monolayer MoS₂ continuous films, *ACS Nano*, **11**: 12001–12007, <https://doi.org/10.1021/acsnano.7b03819>.
65. YUAN Z., YANG C., GAO H., QIN W., MENG F. (2021), High response formic acid gas sensor based on MoS₂ nanosheets, *IEEE Transactions on Nanotechnology*, **20**: 177–184, <https://doi.org/10.1109/TNANO.2021.3059622>.
66. ZHANG S.-L., CHOI H.-H., YUE H.-Y., YANG W.-C. (2014), Controlled exfoliation of molybdenum disulfide for developing thin film humidity sensor, *Current Applied Physics*, **14**(3): 264–268, <https://doi.org/10.1016/j.cap.2013.11.031>.
67. ZHAO G., WU Y., SHAO Y., HAO X. (2016), Large-quantity and continuous preparation of two-dimensional nanosheets, *Nanoscale*, **8**(10): 5407–5411, <https://doi.org/10.1039/C5NR07950K>.
68. ZHOU K.-G., MAO N.-N., WANG H.-X., PENG Y., ZHANG H.-L. (2011), A mixed-solvent strategy for efficient exfoliation of inorganic graphene analogues, *Angewandte Chemie International Edition*, **50**(46): 10839–10842, <https://doi.org/10.1002/anie.201105364>.